High performance vapour-cell frequency standards

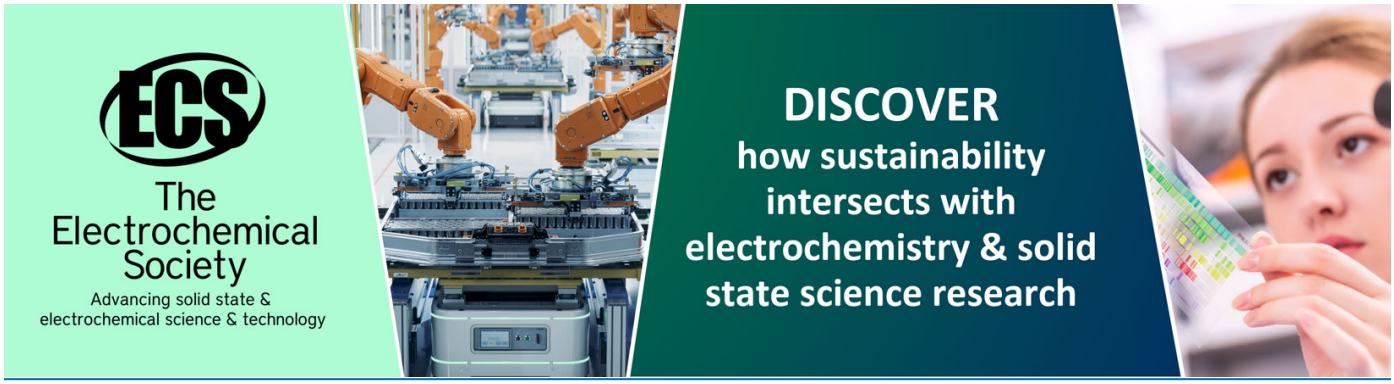

High performance vapour-cell frequency standards

M Gharavipour, C Affolderbach, S Kang, T Bandi, F Gruet, M Pellaton and G Mileti

Laboratoire Temps-Fréquence, Institut de Physique,
Université de Neuchâtel, Switzerland

Email: gaetano.mileti@unine.ch

Abstract. We report our investigations on a compact high-performance rubidium (Rb) vapour-cell clock based on microwave-optical double-resonance (DR). These studies are done in both DR continuous-wave (CW) and Ramsey schemes using the same Physics Package (PP), with the same Rb vapour cell and a magnetron-type cavity with only 45 cm^3 external volume. In the CW-DR scheme, we demonstrate a DR signal with a contrast of 26% and a linewidth of 334 Hz; in Ramsey-DR mode Ramsey signals with higher contrast up to 35% and a linewidth of 160 Hz have been demonstrated. Short-term stabilities of $1.4\times10^{-13}\ \tau^{-1/2}$ and $2.4\times10^{-13}\ \tau^{-1/2}$ are measured for CW-DR and Ramsey-DR schemes, respectively. In the Ramsey-DR operation, thanks to the separation of light and microwave interactions in time, the light-shift effect has been suppressed which allows improving the long-term clock stability as compared to CW-DR operation. Implementations in miniature atomic clocks are considered.

1. Introduction

Since the first invention of lamp-pumped rubidium (Rb) clocks in the 1960's [1,2], the demand for a stable, reliable, and compact Rb frequency standard with low power consumption has been growing, for various applications fields such as industry, telecommunication, navigation, space applications (e.g. GPS [3], GALILEO [4] and COMPASS [5]). Recently, thanks to the semiconductor laser technology, laser-pumped Rb clocks have been considered in several studies, for their better optical pumping efficiency results in short-term frequency stabilities at least one order of magnitude better than their lamp-pumped counterparts [6-9]. This opened up also several new schemes for vapour-cell atomic clocks, such as the continuous-wave (CW) Rb clock [9], coherent population trapping (CPT) Cs clock [10] and pulsed optical pumping (POP) Rb clock [11]. In this paper we report our studies on high-performance Rb frequency standards based on the laser-microwave double-resonance (DR) scheme, using both CW and Ramsey interrogation. Both CW-DR and Ramsey-DR schemes require two resonant electromagnetic fields of light and microwave. In the case of CW-DR, the laser optically pumps the vapour of the Rb atoms by creating a polarization of the atomic ground-state; simultaneously the microwave field, generated from a quartz oscillator and is near-resonant with the ^{87}Rb hyperfine clock transition (energy levels $5^2S_{1/2}\,|\,F_g=1, m_F=0\rangle \leftrightarrow |\,F_g=2, m_F=0\rangle$), is applied. The opacity of the Rb vapour to the transmitted light signal as a function of microwave frequency is a measure of the atomic ground state polarization known as CW-DR signal [9]. In CW-DR, the steps of optical pumping, microwave interrogation and optical detection are applied simultaneously (figure 1(b)). In the case of Ramsey-DR, these three sequences are separated in time, see figure 1(c): first, during optical pumping a strong laser pulse creates a significant atom population imbalance between

the two ground-state levels of ^{87}Rb. Then, in absence of the light, the microwave radiation probes the Rb clock transition using the Ramsey scheme, i.e. by two coherent $\pi/2$ microwave (Rabi) pulses of same pulse duration T_1, amplitude and frequency, but separated by the Ramsey time T_{Ramsey}. Finally, light of same frequency as during optical pumping but with much weaker intensity serves for optical detection and produces a narrow clock-resonance Ramsey signal [12, 13]. The setup design in the case of the CW-DR scheme is less complex with a lower volume and a lower power consumption than in the case of Ramsey-DR. Indeed, this latter requires an acousto-optical-modulator (AOM) that is used as a fast optical switch. However, in the case of the Ramsey-DR scheme, the light shifts (LS) effect (see section 3.3) can be suppressed, thanks to the separation of the light-atom and microwave-atom interactions. Furthermore, the durations and intensities of the optical pumping and detection pulses can be optimized, separately.

2. CW-DR and Ramsey-DR Rb clock setup

The details of our experimental clock setups for both the CW-DR and Ramsey-DR cases were previously presented in [9] and [14, 15] respectively. The same setup (see figure 1(a)) is used for the CW-DR and Ramsey-DR schemes and contains three main components: 1) the frequency-stabilized compact laser head (LH) [16], 2) the Physics Package (PP, containing the Rb cell and magnetron cavity) with an overall volume < 0.8 dm^3, and 3) the local oscillator (LO).

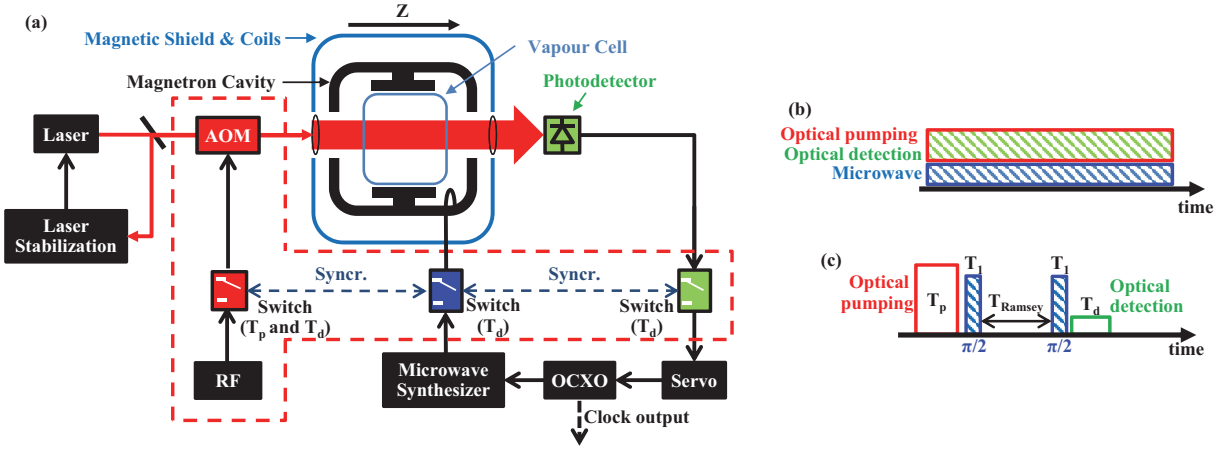

Figure 1. (a) Schematic setup for CW-DR and Ramsey-DR clocks. Components in the dash line are used only in the case of Ramsey-DR scheme. (b) CW-DR sequences. (c) Ramsey-DR sequences. (colour online)

The laser source is a distributed-feedback (DFB) laser diode emitting at 780 nm (Rb D2 transition). Its frequency is stabilized to the sub-Doppler $|5S_{1/2}, F = 1\rangle \rightarrow |5P_{3/2}, F = 1, 2\rangle$ cross-over resonance, using an evacuated ^{87}Rb reference cell that is integrated in the laser-head (LH) assembly [16]. In the case of the Ramsey-DR scheme, an AOM operated in double-pass (not required for CW-DR scheme) is implemented in the LH [17] and serves for: 1) laser output switching to control the durations of the pumping and detection pulses, 2) frequency shifting by -160 MHz, and 3) the control of the laser output power. The PP contains a home-made 25 mm diameter and length glass cell filled with an enriched ^{87}Rb vapour and 26 mbar total buffer-gas pressure (mixture of Argon and Nitrogen, P_{Ar}/P_{N2}=1.6). The cell has a 25 mm long stem acting as a reservoir for the Rb atoms. The Rb vapour cell is placed in a compact magnetron-type cavity with a total external volume of 45 cm^3. The cavity resonates at the ^{87}Rb clock's transition frequency of ≈6.835 GHz, in a TE_{011}-like mode with a relatively low loaded quality factor Q≈200 [18]. This magnetron-type resonator is a good candidate to be also used in the case of Ramsey-DR scheme as it shows a highly uniform microwave magnetic field distribution across the vapour cell. This results in a high contrast Ramsey signal since most of the Rb

atoms experienced well approximated π/2 -pulses [15]. A C-field coil around the resonator generates a static magnetic field (typical amplitude ≈40 mG) oriented parallel to the laser propagation vector (z direction). This static field is required to lift the degeneracy of ^{87}Rb hyperfine ground states into their respective Zeeman levels. A two-layer magnetic shield surrounds the whole system to prevent the external magnetic field fluctuations. The photodetector collects the detection signal after the cell. The LO consists of an oven controlled crystal oscillator (OCXO), the microwave synthesizer to generate the ≈6.835 GHz radiation for ^{87}Rb clock transition interrogation and the servo loop [19].

3. Experimental Results

3.1. DR and Ramsey signals

As explained in the previous section, in the case of the CW-DR scheme both resonant optical and microwave fields act simultaneously (figure 1(b)). The light power transmitted through the cell (as function of the microwave frequency) constitutes the clock signal used to adjust the frequency of the LO. For this scheme the optimized DR signal is shown by the solid red line in figure 2. Here, the laser intensity is 0.46 μW/mm^2 and the microwave input power is -34 dBm. The signal can be well fitted by a Lorentzian line shape with a full width at half maximum (FWHM) $\Delta\nu_{1/2}$=334 Hz, which is limited by optical and microwave power broadening, and a contrast of C=26% [9].

The pulse sequences for the case of the Ramsey-DR scheme are shown in figure 1(c), using the following parameters: 1) optical pumping pulse time T_p=0.4 ms with a laser power of about 15 mW, 2) two π/2 microwave pulses with the duration of T_1=0.4 ms and input power (to the cavity) of –20 dBm, 3) Ramsey time T_{Ramsey}=3 ms, and 4) optical detection pulse time of T_d=0.7 ms with a laser power of about 0.1 mW. The Ramsey pattern obtained in this situation is given by the dashed blue line in figure 2. Its central fringe has a contrast of C=35% and a linewidth of $\Delta\nu_{1/2}$=160 Hz, consistent with the theoretical prediction of $\Delta\nu_{1/2}=1/(2\cdot T_{Ramsey})$ [15].

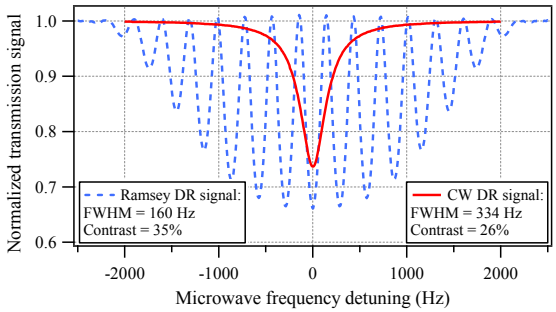

Figure 2. Double resonance signal in the case of the CW-DR scheme (solid red line) compared to Ramsey fringes in the case of Ramsey-DR (dashed blue line) [9, 15]. (colour online)

3.2. Short-term clock stability

The signal-to-noise ratio (S/N) limits the short-term stability (at τ=1 to 100 s) of a passive Rb clock and can be estimated by [9]:

$$\sigma_{S/N}(\tau)=\frac{N_{psd}}{\sqrt{2}\cdot D\cdot\nu_{Rb}}\tau^{-1/2}, \qquad (1)$$

where N_{psd} is the power-spectral density of the detection noise when microwave and pump laser are switched on (in closed-loop condition) and D is the discriminator slope of the error signal. Here, N_{psd} includes shot-noise, laser's amplitude-modulation (AM) noise and FM-to-AM noise conversion in the vapour cell [20]. Moreover, in the case of the Ramsey-DR scheme, contributions of AOM's additional noises are also added [15]. For the CW-DR scheme the clock's shot-noise limit is estimated as $4.9\times10^{-14}\ \tau^{-1/2}$, by replacing N_{psd} in (1) with the shot-noise level. In the Ramsey-DR scheme with optical detection the shot-noise limit can be estimated by [11]:

$$\sigma_{sn}(\tau) = \frac{1}{\pi Q_a R_{sn}} \sqrt{\frac{T_c}{\tau}}, \quad (2)$$

where $Q_a \approx 4.3\times10^7$ is the quality factor of the clock transition and $T_c = 4.95$ ms is the cycle time of the pulse sequence. The signal-to-noise ratio R_{sn} for our clock is at the level of 30000 [14] and the final expected shot-noise stability limit is $\sigma_{sn}(\tau) \approx 1.7\times10^{-14}\ \tau^{-1/2}$.

The total short-term clock stability of $\sigma_y(\tau)$ includes, in addition to the S/N limit, the contributions from the LO's phase noise through the Dick effect [21] and from laser intensity and frequency fluctuations via the light-shifts (LS), and can be expressed as [7]:

$$\sigma_y(\tau) = \sqrt{\sigma^2_{S/N}(\tau) + \sigma^2_{Dick}(\tau) + \sigma^2_{LS}(\tau)}. \quad (3)$$

Table 1 shows the measured short-term instability budget for both CW-DR and Ramsey-DR schemes. The dominant source for this stability is the optical detection noise which mainly originates from the technical laser noise and FM-to-AM noise conversion in the cell [15, 18].

Table 1. Short-term instability budget comparison for both CW-DR and Ramsey-DR Rb clocks.

Instability	**Shot-noise limit ($\tau^{-1/2}$)**	Signal-to-noise $\sigma_{S/N}$ ($\tau^{-1/2}$)	Dick effect ($\tau^{-1/2}$)	Light Shift ($\tau^{-1/2}$)	**Total ($\tau^{-1/2}$) (theory)**	**Total ($\tau^{-1/2}$) (measured)**
CW-DR [9]	$\mathbf{4.9\times10^{-14}}$	1.2×10^{-13}	7.5×10^{-14}	4×10^{-14}	$\mathbf{1.4\times10^{-13}}$	$\mathbf{1.4\times10^{-13}}$
Ramsey-DR [17]	$\mathbf{1.7\times10^{-14}}$	2.0×10^{-13}	$\leq1\times10^{-13}$	3×10^{-15}	$\mathbf{2.2\times10^{-13}}$	$\mathbf{2.4\times10^{-13}}$

3.3. Light shifts (LS)

Light shifts (or AC Stark shifts) are the shifts of the atomic energy levels arising when a near-resonant optical field interacts with an atom [22, 23]. With the clock frequency ν_{clock}, we define the intensity LS coefficient $\alpha=\delta\nu_{clock}/\delta I_L$ (at fixed laser frequency ν_L) and the frequency LS coefficient $\beta=\delta\nu_{clock}/\delta\nu_L$ (at fixed laser intensity I_L). Measured LS coefficients in the CW-DR scheme are $\alpha=1.0\times10^{-12}$ /% and $\beta=1.2\times10^{-11}$ /MHz [9], more than one order of magnitude higher than $\alpha=-2.1\times10^{-14}$/% and $\beta=4.6\times10^{-13}$ /MHz in the Ramsey-DR case [17]. In principle, LS can be fully suppressed in a Ramsey scheme. The residual LSs found in Ramsey-DR mode might be due to the position shift effect (non-uniform spatial distribution of microwave field and laser absorption rate) [12], residual coherence at the beginning of the first Ramsey pulse [24] and residual non-zero light power during the Ramsey phase.

3.4. Microwave power shift (PS)

In both cases of optical-microwave DR interrogation schemes, the spatial inhomogeneity of the optical and microwave fields as well as the residual gradients of the static magnetic field can cause a position dependent inhomogeneous shift on the clock hyperfine frequency. This depends on the microwave power and is called microwave power shift [25]. The microwave power shift coefficients for CW-DR and Ramsey-DR are measured 2.2×10^{-12} /μW and 1.8×10^{-12} /μW, respectively [9, 17].

3.5. Systematic shifts and long-term clock stability

We evaluate the limitations on the medium- to long term frequency stability of our Rb clocks arising from systematic shifts. The contributions from the main physical perturbations such as intensity and frequency LS, microwave power shift, vapour cell and stem temperature coefficients (TC) are measured. Table 2 summarizes and compares the long-term instability budgets for our CW and Ramsey DR clocks, at $\tau=10^4$ s. Measurements of the long-term frequency stability show that in the case of our current vapour cell with a long stem (25 mm), in both CW and Ramsey schemes the total clock instabilities are limited to $\approx6\times10^{-14}$, mainly because of the stem temperature coefficient (TC), although in Ramsey-DR scheme the instability contributions due to LS are reduced by more than one

order of magnitude compared to the CW-DR scheme (from 3.8×10^{-14} to 2.3×10^{-15}). Therefore a new vapour cell with ten times smaller stem volume was designed, resulting in its potential instability contribution reduced to 5.5×10^{-15}. With this cell, we expect our Ramsey-DR clock to reach 7.2×10^{-15} at $\tau=10^4$ s.

Table 2. Comparison of clock stability limitations at $\tau = 10^4$ s, calculated from the main systematic shift coefficients and parameters instabilities.

Effect or source	**CW-DR**		**Ramsey-DR**	
	Long stem [9]	Short stem	Long stem [17]	Short stem
Intensity LS	9.9×10^{-15}		1.1×10^{-15}	
Frequency LS	3.7×10^{-14}		2×10^{-15}	
Cell TC	$\leq 3.5\times10^{-15}$		$\leq 3.5\times10^{-15}$	
Microwave PS	8.9×10^{-16}		1.9×10^{-15}	
Stem TC	5.6×10^{-14}	5.5×10^{-15}	5.6×10^{-14}	5.5×10^{-15}
Total $\sigma_{tot}=[\Sigma_i \sigma_i^2]^{1/2}$	$\mathbf{6.8\times10^{-14}}$	$\mathbf{3.9\times10^{-14}}$	$\mathbf{5.6\times10^{-14}}$	$\mathbf{7.2\times10^{-15}}$
Total (measured)	$\mathbf{6\times10^{-14}}$	**----**	$\mathbf{6\times10^{-14}}$	**----**

4. Applications in miniature DR clocks

The suppression of light-shift effects in the Ramsey-DR scheme could also be beneficial for improving the long-term stability of miniature or chip-scale atomic clocks [26]. We therefore investigate on the approach of Ramsey-mode operation of a miniature DR clock as e.g. described in [27], based on a 50 mm^3 internal volume microfabricated Rb cell and a micro-loop-gap resonator, by numerical simulations using the model described in [15]. First results show that Ramsey signals with a narrow central fringe (760 Hz FWHM) and > 30% contrast may be expected. Such a miniature Ramsey DR clock could be a good candidate for achieving short-term stabilities of $\leq 1\times10^{-11}\ \tau^{-1/2}$ and $< 1\times10^{-12}$ at one day, for e.g. applications such as in smart grids.

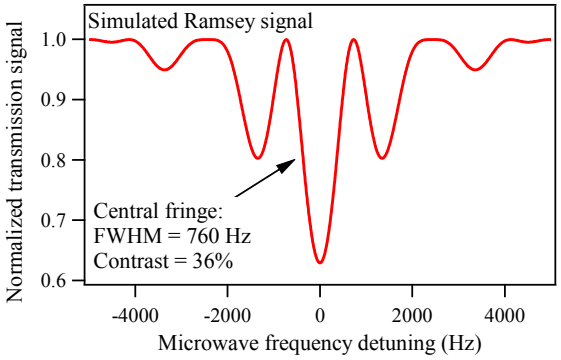

Figure 3: Ramsey DR signal simulated for a micro-fabricated Rb vapour cell such as used in [27]. T_{Ramsey}=0.2ms and T_1=0.4ms. (colour online)

5. Conclusion

We have studied compact Rb atomic clocks based on both CW-DR and Ramsey-DR schemes, using the same clock setup with a clock resonator Physics Package of only 0.8 litres overall volume. CW-DR and Ramsey signals with contrasts of 26% and 35%, and FWHMs of 334 Hz and 160 Hz, respectively, are shown. The measured short-term clock stabilities are $\approx 2\times10^{-13}\ \tau^{-1/2}$ (at τ=1 to 100 s) in both schemes, with optical detection noise being the main limitation. On medium- to long-term scales ($\tau\approx10^4$ s) the main limiting effects in the CW-DR scheme are the LS and stem TC, which can be reduced by about one order of magnitude by passing to the Ramsey-DR scheme and implementing a new cell design, respectively. A final clock stability of $< 1\times10^{-14}$ at 10^4 s up to 1 day is expected.

Acknowledgments
This work was supported by the Swiss National Science Foundation (SNSF grant no. 140712) and the European Metrology Research Programme (EMRP project IND55-Mclocks). The EMRP is jointly funded by the EMRP participating countries within EURAMET and the European Union. We also acknowledge previous support from the European Space Agency (ESA) and the Swiss Space Office (Swiss Confederation). We thank A. K. Skrivervik, C. Stefanucci (both EPFL-LEMA) for their support on the microwave cavity, and C. Calosso (INRIM, Italy) for the microwave LO.

References
[1] Camparo J 2007 *Phys. Today*, **60** 33
[2] Kastler A 1950 *J. Phys. Radium*, **11** 255
[3] Dupuis R T, Lynch T J and Vaccaro J R 2008 *Proc. IEEE Int. Frequency Control Symposium* edited by Jadusliwer B. *(Honolulu, Hawaii, USA 19-21 May 2008)* pp. 655-660
[4] Waller P, Gonzalez S, Binda S, Sesia I, Hidalgo I, Tobias G and Tavella P 2010 *IEEE Trans. Ultrason. Ferroelct. Freq. Control* **57** 738
[5] Chunhao H, Zhiwu C, Yuting L, Li L, Shenghong X, Lingfeng Z and Xianglei W 2013, *Int. J. Navig. Observ.* **2013** 371450
[6] Camparo J and Frueholz 1986 *J. Appl. Phys*. **59** 3313
[7] Mileti G, Deng J, Walls F, Jennings D and Drullinger R 1998 *IEEE J. Quantum Electron.* **34** 233
[8] Vanier J 2005 *Appl. Phys.* B **81** 421
[9] Bandi T, Affolderbach C, Stefanucci C, Merli F, Skrivervik A K and Mileti G 2014 *Ultrasonics, Ferroelectrics, and Frequency Control, IEEE Transactions on* **61** 1769-1778
[10] Danet J M, Kozlova O, Yun P, Guérandel S and De Clercq E 2014 *EPJ Web of Conf.* **77** 00017
[11] Micalizio S, Calosso C E, Godone A and Levi F 2012 , Metrologia **49** 425-436
[12] Micalizio S, Godone A, Levi F and Calosso C 2009 *Phys. Rev.* A. **79** 013403
[13] Godone A, Micalizio S, Levi F and Calosso C 2006 *Phys. Rev.* A **74** 043401
[14] Kang S, Affolderbach C, Gruet F, Gharavipour M, Calosso C E and Mileti G 2014 *Proc. 26th European Frequency and Time Forum (EFTF) (Neuchatel, Switzerland, 23-26 June 2014)* pp. 544-547
[15] Kang S, Gharavipour M, Affolderbach C, Gruet F and Mileti G 2015 *J. Appl. Phys.* **117** 104510
[16] Gruet F, Pellaton M, Affolderbach C, Bandi T, Matthey R and Mileti G, 2012 *Proc. Int. Conf. on Space Optics (ICSO) (Ajaccio, Corsica, 9-12 October 2012)* no. 48
[17] Kang S, Gharavipour M, Gruet F, Affolderbach C and Mileti G. 2015 *Proc. Joint Conf. IEEE Int. Frequency Control Symposium & European Frequency and Time Forum (EFTF) (Denver, Colorado, USA 12-16 April 2015)*, pp. 800-803
[18] Stefanucci C, Bandi T, Merli F, Pellaton M, Affolderbach C, Mileti G and Skrivervik A K 2012 *Rev. Sci. Instrum.* **83** 104706
[19] Calosso C E, Micalizio S, Godone A, Bertacco E K and Levi F 2007 *IEEE Trans. Ultrason., Ferroelectr., Freq. Control.* **54** 1731
[20] Camparo J C 1998 *J. Opt. Soc. Am. B* **15** 1177–1186
[21] Deng J Q, Mileti G, Drullinger R E, Jennings D A, and Walls F L 1999, Phys. Rev. A **59** 773
[22] Cohen-Tannoudji C and Barrat J 1961 P *J. Phys. Radium* **22** 329
[23] Mathur B S, Tang H and Happer W 1968 *Phys. Rev.* **171** 11
[24] Godone A, Micalizio S and Levi F 2004 *Phys. Rev.* A **70** 023409
[25] Vanier J and Audoin C 1989 *The Quantum Physics of Atomic Frequency Standards* vol. 1, (Bristol, UK: Adam Hilger)
[26] Knappe S 2008 MEMS atomic clocks, *Comprehensive Microsystems* (vol. 3) ed. Y B Gianchadani et al. (Amsterdam: Elsevier) pp.571-612
[27] Violetti M, Pellaton M, Merli F, Zürcher J–F, Affolderbach C, Mileti G and Skrivervik A K 2014 *IEEE Journal of Sensors* **14** 3193